Revista Ciencia en Desarrollo. Vol. 16 Num. 1 pp. 188 - 199
enero - junio

DOI: 10.19053/uptc.01217488.v16.n1.2025.16794

Artículo de investigación

Computational study of anandamide analogues as ligands for cb1 cannabinoid receptor

Estudio computacional de análogos de anandamida como ligandos para receptores cannabinoides cb1

Lida R. Rojas Bustamante[1]✉, Wilson E. Rozo-Núñez[2]✉, Karen A. Arias Soler[1]✉, Teodorico Castro Ramalho[1]✉, Fabio Mayorga Niño[2]✉ y Agobardo Cárdenas-Chaparro[1] ✉

[1]Grupo de Investigación de Diseño y Síntesis de Sistemas Químicos (DiSi2Quim), Facultad de Ciencias Básicas, Universidad Pedagógica y Tecnológica de Colombia, Tunja, Colombia.
[2]Facultad de Ciencias de la Salud, Universidad Pedagógica y Tecnológica de Colombia, Tunja, Colombia.
[3]Laboratorio de Modelado Molecular, Departamento de Química, Universidad Federal de Lavras, Brasil.

Recepción: 19-nov-2023 **Aceptado:** 28-abril-2024 **Publicado:** 23-julio-2024
Cómo citar: Rojas Bustamante, L. R., Rozo Nuñez, W. E., Arias Soler, K. A., Castro Ramalho, T., Mayorga Niño, F., & Cárdenas Chaparro, A. (2025). Computational study of anandamide analogues as ligands for cb1 cannabinoid receptor. *Ciencia en Desarrollo*, 16(1). doi: 10.19053/uptc.01217488.v16.n1.2025.16794

Abstract

Anandamide, also known as N-arachidonoylethanolamide (AEA), is an endocannabinoid compound synthesized from phospholipids present in cell membranes, including those of the brain and peripheral nervous system. The in-silico study of this compound not only sheds light on the intricate biological mechanisms that govern our physiology, but also promises to unlock new therapeutic strategies to improve quality of life and treat a wide variety of medical disorders. This study focuses on the prediction of the absorption, distribution, metabolism, excretion, and toxicity (ADME/T) processes of AEA and 30 new analogues using computational tools such as SwissADME, ProTox-II and VenomPred. Additionally, the molecular binding of AEA analogues to the human endocannabinoid receptor type 1 (CB1) was evaluated. The results showed that all compounds exhibited acceptable oral bioavailability, and that only two compounds permeate the blood–brain barrier (BBB) (11 and 12). Toxicity data indicated that 26 ligands are in class 4. Molecular docking identified five analogues (10, 23, 24, 29 and 30) with optimal free energy values. This study highlights AEA analogues as compounds with pharmaceutical applications.

Keywords: anandamide, CB1 receptor, molecular docking, ADMET prediction.

Resumen

La anandamida, también conocida como N-araquidonoiletanolamida (AEA), es un compuesto endocanabinoide sintetizado a partir de fosfolípidos presentes en las membranas celulares, incluyendo las del cerebro y el sistema nervioso periférico. El estudio in silico de este compuesto, no sólo arroja luz sobre los intrincados mecanismos biológicos que rigen nuestra fisiología, sino que también promete desbloquear nuevas estrategias terapéuticas para mejorar la calidad de vida y tratar una amplia variedad de trastornos médicos. Este estudio se enfoca en la predicción de los procesos de absorción, distribución, metabolismo, excreción y toxicidad (ADMET) de la AEA y 30 nuevos análogos utilizando herramientas computacionales como SwissADME, ProTox-II y VenomPred. Adicionalmente, se evaluó el acoplamiento molecular de los análogos de AEA con el receptor endocannabinoide humano tipo 1 (CB1). Los resultados arrojaron que todos los compuestos exhibieron una biodisponibilidad oral aceptable y que sólo dos compuestos permean la membrana hematoencefálica (11 y 12). Los datos de toxicidad indican que 26 ligandos se encuentran en clase 4. Por otro lado, el acoplamiento molecular identificó cinco análogos (10, 23, 24, 29 y 30) con valores óptimos de energía libre. Este estudio destaca a los análogos de AEA como compuestos con aplicaciones farmacéuticas.

Palabras Clave: anandamida, receptor CB1, docking molecular, predicción ADMET.

E-ISSN: 2462-7658

1 Introduction

Endocannabinoids (eCBs) are molecules produced by the body, essential in the maintenance of internal balance, known as homeostasis. As well, they are the most abundant neuromodulators and are produced from arachidonic acid (AA) [1]. One of the main eCBs is anandamide (Figure 1), a polyunsaturated and fat-soluble compound that contains an amide-type bond in its structure that acts as a hydrogen acceptor [2], AEA mainly activates cannabinoid receptors (CB1 and CB2). In this work, the CB1 receptor is evaluated due to its a wide distribution in the human body and AEA is the ligand with the highest affinity to them, due to the polar ethanolamino group of the anandamide and the carboxylic group of the receptor forming hydrogen bonds. The hydrophobic interaction of the AEA molecule is also involved in the activation of CB1. In addition, they modulate a variety of pathophysiological effects as well as neurobiological processes of addiction, cell death, reproduction and immune response [3].

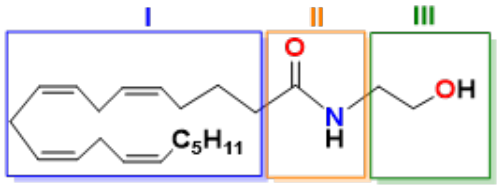

Figure 1: AEA structure and potential pharmacophoric points. I: hydrocarbon chain, II: carboxamide group and III: polar group at the end of the molecule.

A key function of anandamide is to mediate cell death and induce apoptosis. A mechanism used by our body to eliminate mutated cells and aberrant replications. For this reason, AEA analogues have been developed with significant inhibitory action on the proliferation of different types of cancers in humans such as prostate, breast, lung, kidney, among others [4–8].

Likewise, compounds analogous to AEA have been developed as a palliative in Parkinson's disease [9], and stress regulation [10], with anti-inflammatory effects as analgesic strategies for asthma and migraine [11]. However, when AEA is administered pharmacologically, it causes psychoactive effects, due to its lipophilic character, which facilitates permeability at the blood-brain membrane (BBB) [12, 13]. In addition, numerous AEA analogues, already synthesized and evaluated, show problems such as poor water solubility and high flexibility generating different biological conformations [14]. Therefore, drug design aims to obtain more water-soluble AEA analogues that avoid adverse effects.

On the other hand, the search and design of new drugs is a highly complex and costly process, due to the multiple stages that must be carried out before approval is obtained. It is precisely for this reason that the use of Computer-Aided Drug Design (CADD) tools in the pharmaceutical industry has currently gained great relevance. This approach integrates chemical-computational strategies that not only accelerate the process, but also improve the traditional methodology of search, synthesis and evaluation of the biological activity of new chemical compounds [15].

The use of CADD in the early stages of drug development allows for significant cost and time optimization. This is interpreted as the ability to screen a previously unimaginable number of structures, from thousands to millions of compounds. As a result, the probability of identifying successful ligands that can be synthesized, purified, and tested in clinical trials is substantially increased. Within the CADD methodology, there are several studies, such as, virtual ligand screening, where the prediction of Administration, Digestion, Metabolism, Excretion and Toxicity (ADMET) properties is made [16, 17], Lipinski tests [18] and molecular docking [19]; which give an insight into how these compounds would behave in the organism before starting the experimental synthesis process [20]. There is another important parameter in drug design that allows selecting the most promising virtual molecules that will be synthetized and submitted to biological assays. Synthetic accessibility (SA) is a key factor in this selection process. The SA score ranges from 1 (easy synthesis) and 10 (difficult synthesis) [18].

In this work, a design of 30 anandamide analogs was carried out with a virtual ligand screening where a prediction of ADMET properties was made, and a molecular docking study, where the affinity to the human CB1 receptor, was evaluated.

2 Experimental

2.1 AEA Analogue Design

Anandamide analog molecules with potential antineoplastic action were designed. This design was based on previous research and considered aspects of medicinal chemistry and molecular pharmacology, such as the pharmacophore group of AEA and increase of polarity, likely to mitigate psychoactive effects. The ethanolamide fragment from the AEA molecule was maintained by including bioisosteric groups, such as aliphatic terminations between 4 and 7 carbons, which have shown good flexibility at the active site of the CB1 receptor. To generate more conformationally restricted analogs, phenolic-type aromatic rings that are involved in a close relationship with the CB1 receptor were incorporated into the structures [21]. Furthermore, several alternatives involving chemo and enantioselectivity were designed, as shown in Figure 2.

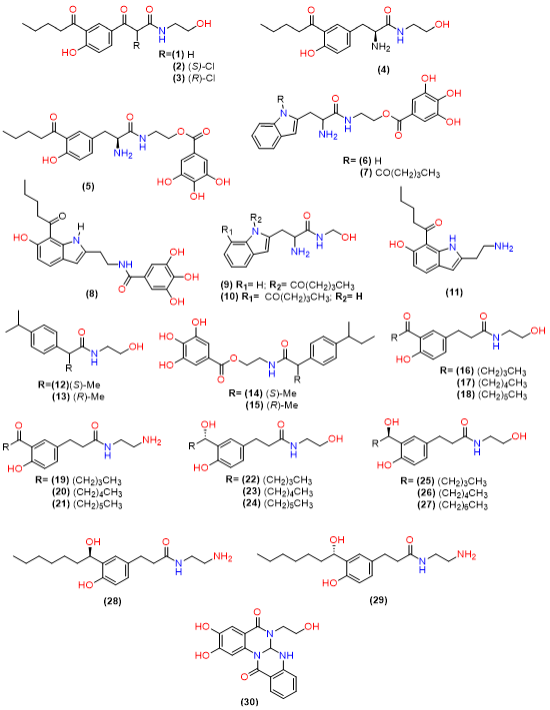

Figure 2: Structure of designed AEA analogues.

2.2 ADMET forecast

The theoretical simulation study of ADME properties was developed with the freely available web tool Swiss Institute of Bioinformatics (SwissADME) [22]. First the molecules were drawn using the ACD/ChemSketch software, and the SMILE code of the 30 molecules was generated. Properties such as lipophilicity, water solubility, pharmacokinetics and drug similarity were calculated. To assess toxicity, the Protox-II and Venompred tools [17], were used, which provide predictions of toxicity class and categories, including mutagenicity, tumorigenicity, irritation, reproductive effects, hepatotoxicity,

carcinogenicity and cytotoxicity.

2.3 Molecular docking

The 3D structures of the composites were constructed and optimized using Gaussian 09 software [23], and the partial charges of the atoms were elucidated. The compounds were fully optimized at the DFT level, with density functional B3LYP and 6-31G (d, p) basis set, using the CHELPG methodology [24]. The crystallographic structure of the macromolecular target, the human cannabinoid receptor (CB1) was extracted from the Protein Data Bank with PDB code: 5TGZ and a resolution: of 2.8 Å [25].

Once the protein and ligands were prepared, molecular docking of the proposed ligands was performed (Figure 3). Docking studies were then performed using the Molegro Virtual Docker (MVD®) [26], considering the same procedures used previously. For best results, amino acid residues within 5 Å were kept flexible. Give the nature of the docking methods, calculations were run, generating 50 poses (conformation and orientation) for the ligand.

The MolDock scoring function employed in the MVD program comes from the piecewise linear potential (PLP), a simplified potential whose parameters are fitted to protein-ligand structures, binding data scoring functions and further extended in the Generic Evolutionary Method for molecular docking with a new hydrogen bonding term and new charge schemes [27]. The values of the docking score function, E_{score}, are defined by Eq. 1:

$$E_{\text{score}} = E_{\text{inter}} + E_{\text{intra}} \tag{1}$$

where E_{inter} is the intermolecular interaction energy of the protein-ligand complex and E_{intra} is the internal energy of the ligand. The E_{inter} term is shown in Eq. 2:

$$E_{\text{inter}} = \sum_{i \in \text{ligand}} \sum_{j \in \text{protein}} \left[E_{\text{PLP}}(r_{ij}) + \frac{332.0\, q_i q_j}{4 r_{ij}^2} \right] \tag{2}$$

The term E_{PLP} represents the PLP (Piecewise Linear Potential) energy consisting of two sets of parameters: one for approximating the steric term (Van der Waals) between atoms, and another for hydrogen bonding.

The second term, $332.0 \frac{q_i q_j}{4 r_{ij}^2}$, corresponds to electrostatic interactions between charged atoms. It is a Coulomb potential with a distance-dependent dielectric constant ($D(r) = 4r$). The factor 332.0 ensures that the electrostatic energy is expressed in kilocalories per mole. Here, q_i and q_j are the charges of atoms i and j, and r_{ij} is the interatomic distance between them [28].

The E_{intra} term is presented in Eq 3:

$$E_{\text{intra}} = \sum_{i \in \text{ligand}} \sum_{j \in \text{ligand}} E_{\text{PLP}}(r_{ij}) + \sum_{\text{Flexible bonds}} A\,[1 - \cos\cos(m\theta - \theta_0)] + E_{\text{clash}} \tag{3}$$

The first part of the equation (double summation) covers all pairs of atoms in the ligand, excluding those connected by two bonds. The second term represents the torsional energy, where θ is the torsional angle and θ_0 is its equilibrium value. The last term, E_{clash}, applies a penalty of 1000 if the distance between two heavy atoms (not directly bonded) is less than 2.0 Å, thus filtering out non-viable ligand conformations.

The docking search algorithm used in the MVD program is based on an evolutionary algorithm—an optimization technique inspired by Darwinian theory—and a hybrid search algorithm known as guided differential evolution. This hybrid combines differential evolutionary optimization with a cavity prediction algorithm during the search process, enabling fast and accurate identification of potential binding modes (poses) [29].

3 Results and Discussion

3.1 ADMET Analysis

The results of ADME of the 30 compounds, physicochemical properties, lipophilicity, solubility, pharmacokinetic and skin permeability parameters are listed in the annexes (Table S1).

The lipophilicity data of the 30 compounds expressed as the logarithm of the octanol-water partition coefficient (Log Po/w), are shown in figure 3. (Table S1). All compounds exhibit a value of Log Po/w < 5, which agrees with Lipinski's principle. Within this set, compound 14 stands out as the most lipophilic with a Log Po/w of 3.11; while compound 30 shows the lowest degree of lipophilicity, with a Log Po/w of 0.43, indicating a higher hydrophilicity.

These lipophilicity data suggest that the more lipophilic a compound is, the greater its propensity to cross biological membranes, such as the intestinal barrier and the blood-brain barrier, which, in turn, indicates its ability to be absorbed into the bloodstream and effectively distributed to various tissues and organs. Lipophilicity emerges as a critical property that provides valuable information about the absorption, distribution, metabolism and excretion of a molecule in the body [30].

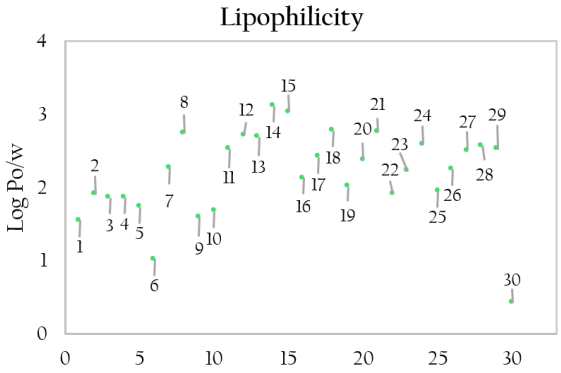

Figure 3: Lipophilicity values of the 30 compounds studied.

Figure 4. shows the solubility results according to SWISSADME in three predictive models like ESOL (Estimated SOLubility) [31], solubility adapted by Ali et al. [32] and SILICO-IT methods. The ESOL method calculates the water solubility directly from the molecular structure talking into account its weight [31] using a solubility scale (Log S) insoluble < -10, poor < -6, moderate < -4, soluble < -2 and high < 0. By this method, most of the molecules showed high solubility, where the most soluble compound was compound 10 (Log S: -2.29) and the ligands, 8 (Log S: -4.38), 14 (Log -4.41) and 15 (Log -4.41) showed moderate solubility between the range of -4.38 and -4.41.

Based on the Ali method, which considers the effect of the topological polar surface area (TPSA), which is a measure that provides information about the polarity of a molecule, estimate the solubility in water [33] and scales within the range of, lower solubility -5.42 < Log S < -3.57 higher water solubility. Taking these parameters into account, 15 of the 30 compounds showed water solubility, with compound 9 with Log S: -3.05 being the most soluble, and compound 8 Log S: -6.19, being the least soluble.

Finally, the solubility results obtained through the SILICO-IT method

reveal a fragmented process with water solubility values in the range of -8.33 < Log S < - 4.28 [34]. The results reveal that only four compounds show good solubility, compounds 1 (Log S: -3.95), 9 (Log S: -3.91), 25 (Log S: -3.93), and 30 (Log S: -3.06). These results provide estimates of the compounds in water, where all 30 ligands are soluble to moderately soluble, which is important in pharmaceutical, and chemical applications (Table S2).

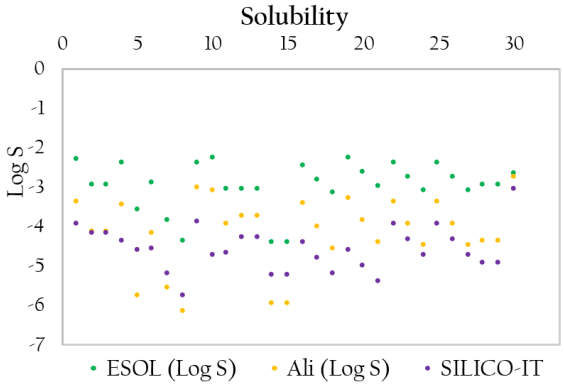

Figure 4: Solubility values of the 30 compounds studied in ESOL, Ali and SILICO-IT models.

The predicted pharmacokinetic parameters of gastrointestinal (GI) absorption, P-gp substrate and cytochrome P450 (CYP) inhibition or interaction for all 30 compounds are presented in Figure 5 (Table S3) taking Log Po/w and TPSA into account. While Log P relates to the affinity of a molecule for lipid substances and its ability to cross membranes composed mostly of lipids, TPSA focuses on the polarity of a molecule and its ability to interact with polar solvents and biological entities such as proteins. These two properties play a fundamental role in the design and understanding of the activity of chemical compounds in pharmaceutical applications and medicinal chemistry.

Therefore, the data obtained for passive human gastrointestinal (GI) absorption indicate that 87% (molecules inside the blue circle) of the 30 molecules studied present high absorption in the digestive tract, while the remaining 13% (5-8) (molecules outside the blue circle) show lower absorption. Moreover, only two compounds (11 and 12) (molecules inside the yellow circle) were observed to have the ability to cross the blood-brain barrier. This indicates that, give the highly elaborated structure and semi-permeable membrane properties, the gastrointestinal (GI) barrier, gives fat-soluble molecules to penetrate through it by diffusion [34].

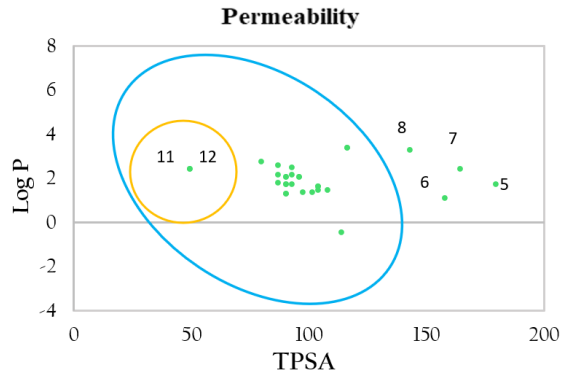

Figure 5: BOILED-Egg Diagram [35] of the 30 compounds. molecules within the blue oval indicate GI permeability and within the yellow circle blood-brain barrier (BBB) permeability.

It is also important to determine whether the compounds are substrates of P-glycoprotein (P-gp), a permeable protein whose function is to expel substances from the body and prevent their absorption [36]. According to (Figure 6), it was observed that 50% of the compounds behave as P-gp substrates, while the other 50% do not. This distinction has significant implications for the absorption, distribution and elimination of these compounds in the body.

In addition, it is essential to understand the interaction of molecules with cytochromes P450 (CYP). These isoenzymes are key in the elimination of drugs by metabolic biotransformation, as they can synergistically process small molecules to enhance tissue and organ protection [37]. The main enzyme isoforms CYP1A2, CYP2C19, CYP2C9, CYP2D6 and CYP3A4 [38] (Figure 6), which are involved in drug metabolism, and inhibitors block their metabolic activity in a dose-dependent manner.

Compounds 11, 12 and 30, demonstrated their ability as inhibitors of the CYP1A2 enzyme. As for the CYP2C19 enzyme, none of the compounds exhibited inhibitory activity. On the other hand, compound 14 was identified as an inhibitor of the CYP2C9 enzyme, while compounds 8, 11-13, 20, 21, 26, and 28 showed their ability to inhibit the CYP2D6 enzyme. Finally, in relation to the CYP3A4 enzyme, only compound 21 exhibited inhibitory activity.

These results are indicative of the compounds ability to interfere with the activity of these enzymes. This interference could have a significant impact on the metabolism of other drugs, which could affect both their efficacies and side effect profiles; which, in turn, could increase their toxicity potentials. These effects differ from those observed with other compounds that do not show inhibitory activity and do not interfere with enzymes of the CYP liver metabolism system, as illustrated in (Figure 6).

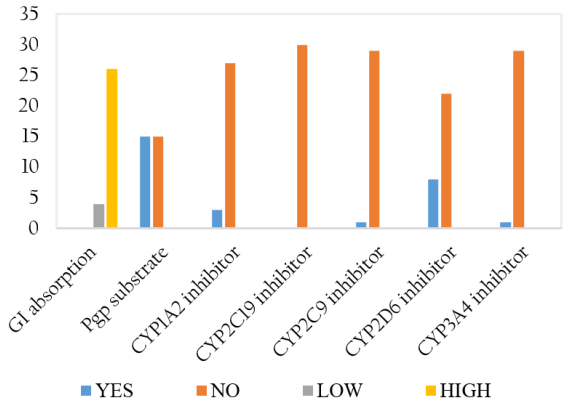

Figure 6: Pharmacokinetic properties, gastrointestinal absorption, PGP substrate and P450 coenzyme inhibitors.

Another method of drug administration is through the skin by transdermal distribution. This approach facilitates the transport of substances or molecules through the epidermis, and its efficacy is studied by the skin permeability coefficient (Kp). A more negative log Kp value (with Kp in cm/s) indicates a lower permeability of the molecule. In this context, compound 30 has a lower permeability compared to the more permeable compounds 12 and, 13, as shown in (Figure 7), because it has a lower molecular weight compared to the other compounds, which facilitates its distribution in the bloodstream. In the context of drug delivery, it is sometimes desirable for a molecule to be permeable through the skin or biologicalmembranes, as this can facilitate its absorption into the bloodstream and distribution in the body.

Similarity to Lipinski's (Pfizer) standards-based medicines [18], Veber (GSK) [39], Ghose (Amgen) [40], Muegge (Bayer) [41] and Egan (Pharmacia) [42], as well as the bioavailability score were assessed.

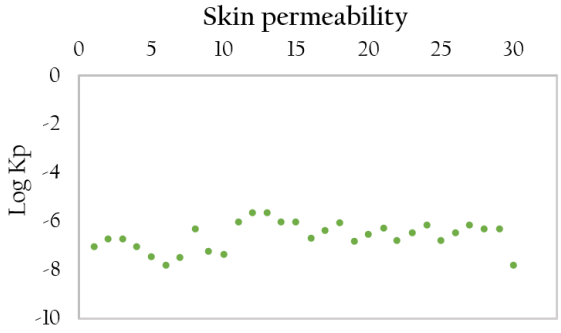

Figure 7: Skin permeability of the 30 compounds.

These filters help to qualitatively define the viability of a compound to become a potential drug candidate for oral administration (Table S4).

Compounds (5, 6, and 8) present a violation of Lipinski's rules since they have more than 5 hydrogen bond donor groups (HBD) in their structure, which has a negative impact on bioavailability and influences their efficacy as potential drugs. The significant affinity for water also predisposes them to establish solid hydrogen bonds in the digestive system. This phenomenon results in accelerated elimination of the compound in the gastrointestinal tract, which prevents adequate absorption into the bloodstream. As a result, the bioavailability of the compound is negatively affected, as an insufficient amount of the drug reaches the systemic circulation to produce the desired therapeutic effect [43].

According to Veber's methods, 15 compounds were non-compliant in some cases by TPSA > 140, rotatable bonds > 10, or both. Based on Ghose's methods, compounds 7 and 30 were non-compliant with the MW > 480 g/mol rule. Compounds 5 and 6 have a TPSA>150 and H-don > 5, compound 7 has a TPSA>150, and 8 has H-don > 5 which fails to comply with Muegge's rules. Finally, Egan's filter indicated that compounds 5-8 violate a rule since they have a TPSA> 131.6 (Figure 8). In terms of oral bioavailability, all compounds have a value of 0.55, indicating that 55% of the administered compound is absorbed into the systemic circulation and is available to act in the body. This result is acceptable for many drugs and compounds. [43].

Toxicity results from the Protox-II program indicated that out of the 30 compounds, 9 and 11 are in class 3 toxicity which are toxic if ingested (50 mg/kg < LD50 ≤ 300 mg/kg). The ligans 14 and 15 are found in class 5, indicating that they may be harmful if ingested (2000 mg/kg < LD50 ≤ 5000 mg/kg), and the rest of the compounds have a toxicity class 4 which makes them harmful if ingested (300 mg/kg < LD50 ≤ 2000 mg/kg). The latter two classes indicate that a higher amount of compound is required to be toxic or harmful to the organism but are generally not lethal [17]. Figure 8 shows the toxicity results according to the ProTox-II and VenomPred programmes, showing that only ligand 4 presents a high probability of hepatotoxic activity with a value of 0.69. These results indicate that they do not present any risk to the organism in terms of carcinogenicity, mutagenicity, and cytotoxicity, suggesting that they could be administered orally (Table S5) [18].

Figure 8: Probability of activity (red) and inactivity (high dark green and low light green), by type of toxicity. A) Hepatotoxicity, B) Carcinogenicity, C) Mutagenicity and D) Cytotoxicity.

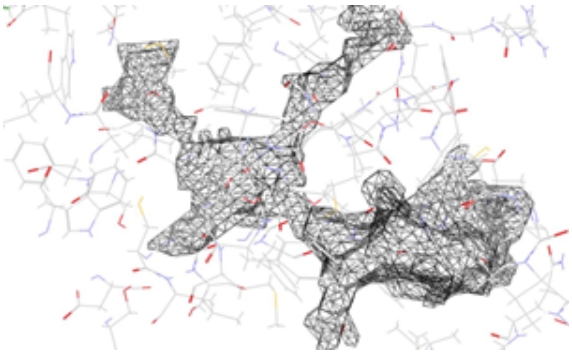

Figure 9: Active site cavity volume = 420.864 Å.

3.2 Molecular docking

Initially, to carry out the docking procedure, a 3D box-based cavity prediction algorithm was used to generate CB1 receptor binding sites via the Molegro Virtual Docker program. The cavity volume was 420.864 Å (Figure 9).

Once the protein was prepared in the MVD and the compounds (ligands 1-30) in Gaussian 09, docking was carried out where the MVD scoring function assigned a binding free energy value to each of the protein-ligand complexes. These energies helped to elucidate the electronic and structural aspects of the binding mode of the ligands in the active site of each protein. All 30 designed molecules indicated good affinity results for the CB1 receptor (Table S6).

Figure 10 shows that the best ligand-receptor interaction energy results correspond to compounds 30 (-118.91 kcal/mol), 23 (-104.45 kcal/mol), 24 (- 98.60 kcal/mol), 29 (-97.70 kcal/mol) and 10 (-97.51 kcal/mol). This suggests that these interactions are strong and ther-

modynamically favorable. Given that, the more negative energy values in their interactions with proteins or therapeutic targets suggest stronger binding and potentially greater efficacy as a pharmaceutical.

On the other hand, the only compound with no interaction at the CB1 active site was compound 7, with a positive energy value (4.66Kcal/mol). This indicates that the interaction between this compound and the protein is unfavorable from a thermodynamic point of view. This means that the formation of the bond between the compound and the protein is not spontaneous. In other words, the binding between the compound and the protein is unlikely or unstable.

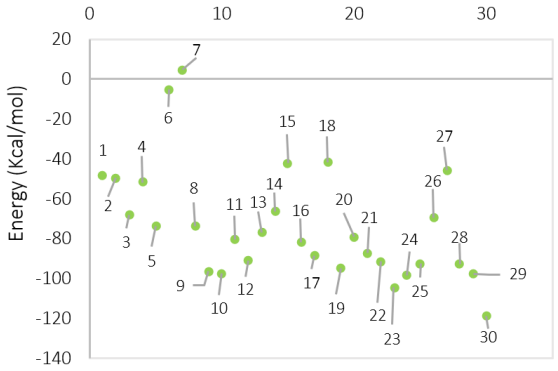

Figure 10: Coupling results expressed in energy (Kcal/mol) of the 30 compounds.

By performing the calculations, it was possible to observe the effect of ligand stereochemistry. For instance, compound 15 established hydrogen bonds with the Thr197 and Ser383 residues of CB1, while compound 14 only bonded with the Ser383 residue, having the best energy value, which reinforces the fact that there are other factors, beyond hydrogen bonds, that contribute significantly to the stabilization of the compound in the active site. The interactions are shown in figure 11.

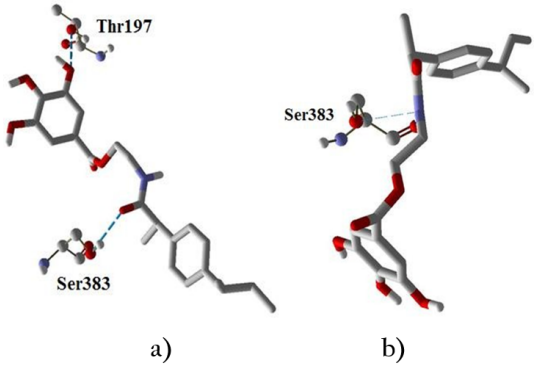

Figure 11: Hydrogen bonds formed by compounds (a) 15 and (b) 14 in the human CB1 receptor.

Compound 7 did not show favorable interactions with the CB1 receptor, despite forming hydrogen bonds with the amino acids, Cys386, Trp279 and Thr197, which were not sufficient to stabilize the compound in the active site, resulting in a positive energy value (4.66 kcal/mol). These interactions are shown in figure 12.

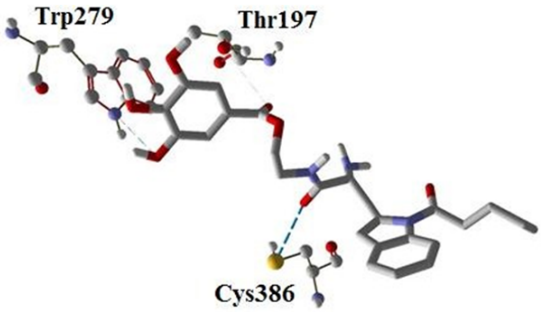

Figure 12: Hydrogen bonds made by Compound 7 at the active site of the human CB1 receptor.

To conclude, compound 30, which the best energy and affinity towards the CB1 receptor presented hydrogen bridge interactions with two amino acid residues, Ile267 and Asp104, as presented in figure 13.

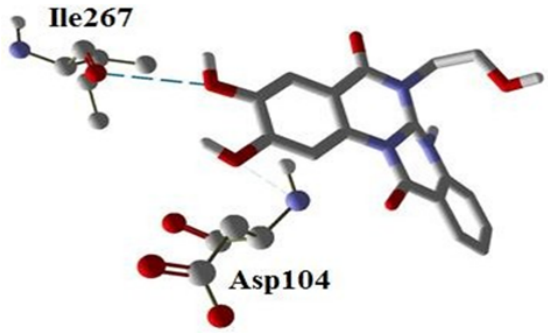

Figure 13: Hydrogen bonds between compound 30 and the active site of human CB1.

3.3 Semi-empirical results: affinity

To complement the molecular docking studies, semi-empirical calculations of PM6 in the CB1 active site were performed for the 5 ligands that presented the best intermolecular interaction energies, considering the electronic contributions of the binding mode of the compounds studied (Table 1).

Table 1: Relative energies calculated using the semi-empirical PM6 method.

Compound	Relative energies of PM6 (kcal/mol)
30	0,00
23	2,96
24	3,58
29	12,20
10	25,40

According to the values described in the table above, the 5 best compounds of the 30 AEA analogs with optimal free energy values are shown, (-118.91 kcal/mol to -97.51 kcal/mol). Compound 30 presented the lowest energy, with respect to the 5 compounds analyzed. However, compounds (23 and 24) showed very close values in energy; unlike compounds (29 and 10) whose energy values were 12.20 and 25.40 kcal/mol respectively, higher than the value found for the compound (30).

4 Conclusions

The following predictions can be drawn from the results of this research.

1. The ADME results showed that all 30 AEA analogs had a Log Po/w < 5, suggesting their ability to cross biological membranes. Compound 14, being the most lipophilic with a Log Po/w of 3.11, has a high potential for absorption and distribution in the organism, while compound 30, with a Log Po/w of 0.43, is more hydrophilic.

2. With respect to similarities with medications, the results showed that most of the compounds meet these criteria, which makes them promising for development as orally administered pharmaceuticals. However, it is important to note that some compounds (5, 6, 7 and 8), break some of these rules, which could influence their bioavailability and therefore require further analysis before considering their use as oral pharmacological candidates.

3. Toxicity predictions revealed that 26 compounds are likely to be inactive, suggesting that these compounds do not pose a significant risk to the organism. Importantly, only two compounds (14 and 15) were classified as toxicity class 5. This implies that they could be harmful if ingested in substantial quantities (with an LD50 between 2000 mg/kg and 5000 mg/kg).

4. The docking calculations showed high affinity towards the human CB1 receptor, but compound 7 did not show favorable interactions with the CB1 receptor. This indicates that the hydrogen bonds made, together with structural and electronic effects, help the proper stabilization of these ligands at the receptor.

5. All the compounds studied reflect good interaction energy scores with CB1, but compounds 30 (118.91 kcal/mol) and 23 (104.45 kcal/mol) had the best values. The PM6 semi-empirical calculations exhibited the same trend found in the docking results, providing some evidence regarding the reactivity of some compounds at the active site of the human CB1

Declaration of competing interest The authors declare that they have no known competing interests that could have appeared to influence the work reported in this paper.

Acknowledgements

The authors acknowledge the support given of Universidad Pedagógica y Tecnológica de Colombia. Tunja-Boyacá, Colombia.

Authorship contribution statement

Lida R. Rojas Bustamante: Writing – original draft, Investigation, Methodology, Validation, Conceptualization. Wilson E. Rozo-Núñez: Writing – review & editing, Resources, Investigation, Conceptualization. Karen A. Arias Soler: Writing – review & editing, Formal análisis, Visualization, Conceptualization. Teodorico Castro Ramalho: Writing – review & editing, Supervision, Investigation, Formal analysis, Conceptualization. Fabio Mayorga Niño: Writing – review &editing, Investigation, Conceptualization. Agobardo Cárdenas-Chaparro: Writing – review & editing, Supervision, Resources, Investigation, Conceptualization.

References

[1] T. Behl, R. Makkar, A. Sehgal, S. Singh, H. Makeen, M. Albratty, et al., "Exploration of Multiverse Activities of Endocannabinoids in Biological Systems," *Int. J. Mol. Sci.*, vol. 23, no. 10, 2022, doi: 10.3390/ijms23105734.

[2] B. Gagestein, A. Stevens, D. Fazio, B. Florea, T. Van der Wel, A. Bakker, *et al.*, "Chemical proteomics reveals off-targets of the anandamide reuptake inhibitor WOBE437," *ACS Chem. Biol.*, vol. 2022, pp. 1174–1183, 2022, doi: 10.1021/acschembio.2c00122.

[3] I. Fernández-Moncada, R. S. Rodrigues, U. B. Fundazuri, L. Bellocchio, and G. Marsicano, "Type-1 cannabinoid receptors and their ever-expanding roles in brain energy processes," *J. Neurochem.*, no. February, pp. 1–11, 2023, doi: 10.1111/jnc.15922.

[4] A. Sobiepanek, M. Milner-Krawczyk, P. Musolf, T. Starecki, and T. Kobiela, "Anandamide-modulated changes in metabolism, glycosylation profile and migration of metastatic melanoma cells," *Cancers*, vol. 14, no. 6, 2022, doi: 10.3390/cancers14061419.

[5] D. Melck, L. De Petrocellis, p. Orlando, T. Bisogno, C. Laezza, M. Bifulco, *et al.*, "Suppression of nerve growth factor Trk receptors and prolactin receptors by endocannabinoids leads to inhibition of human breast and prostate cancer cell proliferation," *Endocrinology*, vol. 141, no. 1, pp. 118–126, 2000, doi: 10.1210/endo.141.1.7239.

[6] C. Ferreri, D. Anagnostopoulos, I. N. Lykakis, C. Chatgilialoglu, and A. Siafaka-Kapadai, "Synthesis of all-trans anandamide: A substrate for fatty acid amide hydrolase with dual effects on rabbit platelet activation," *Bioorg. Med. Chem.*, vol. 16, no. 18, pp. 8359–8365, 2008, doi: 10.1016/j.bmc.2008.08.054.

[7] J. Ravi, A. Sneh, K. Shilo, M. W. Nasser, and R. K. Ganju, "FAAH inhibition enhances anandamide mediated anti-tumorigenic effects in non-small cell lung cancer by downregulating the EGF/EGFR pathway," *Oncotarget*, vol. 5, no. 9, pp. 2475–2486, 2014, doi: 10.18632/oncotarget.1723.

[8] B. S. Tanturovska, R. Manaila, D. Fabbro, and A. Huwiler, "Lipids as Targets for Renal Cell Carcinoma Therapy," 2023.

[9] K. Klatt-Schreiner, L. Valet, J. Kang, A. Khlebtovsky, S. Trautmann, L. Hahnefeld, *et al.*, "High glucosylceramides and low anandamide contribute to sensory loss and pain in Parkinson's disease," *Mov. Disord.*, vol. 35, no. 10, pp. 1822–1833, 2020, doi: 10.1002/mds.28186.

[10] A. Dlugos, E. Childs, K. L. Stuhr, C. J. Hillard, and H. De Wit, "Acute stress increases circulating anandamide and other n-acylethanolamines in healthy humans," *Neuropsychopharmacol.*, vol. 37, no. 11, pp. 2416–2427, 2012, doi: 10.1038/npp.2012.100.

[11] M. McKenna and J. J. McDougall, "Cannabinoid control of neurogenic inflammation," *Br. J. Pharmacol.*, vol. 177, no. 19, pp. 4386–4399, 2020, doi: 10.1111/bph.15208.

[12] C. Silvestri and V. Di Marzo, "The endocannabinoid system in energy homeostasis and the etiopathology of metabolic disorders," *Cell Metab.*, vol. 17, no. 4, pp. 475–490, 2013, doi: 10.1016/j.cmet.2013.03.001.

[13] J. P. M. Basto, E. D. Burgos, D. A. Fandiño, L. F. Porras, D. S. Rodríguez, S. Agudelo, *et al.*, "The bond between the endocannabinoid system and food addiction: A scoping review," *Rev. Esp. Nutr. Hum. Diet.*, vol. 25, no. 2, pp. 212–226, 2021, doi: 10.14306/renhyd.25.2.1153.

[14] J. J. Manning, H. M. Green, M. Glass, and D. B. Finlay, "Pharmacological selection of cannabinoid receptor effectors: Signalling, allosteric modulation and bias," *Neuropharmacology*, vol. 193, no. April, p. 108611, 2021, doi: 10.1016/j.neuropharm.2021.108611.

[15] F. Saldívar-González, F. D. Prieto-Martínez, and J. L. Medina-Franco, "Descubrimiento y desarrollo de fármacos: un enfoque computacional," *Educacion Quimica*, vol. 28, no. 1, pp. 51–58, 2017, doi: 10.1016/j.eq.2016.06.002.

[16] X. Tian, J. Guo, F. Yao, D. P. Yang, and A. Makriyannis, "The conformation, location, and dynamic properties of the endocannabinoid ligand anandamide in a membrane bilayer," *J. Biol. Chem.*, vol. 280, no. 33, pp. 29788–29795, 2005, doi: 10.1074/jbc.M502925200.

[17] P. Banerjee, A. O. Eckert, A. K. Schrey, and R. Preissner, "ProTox-II: A webserver for the prediction of toxicity of chemicals," *Nucleic Acids Research*, vol. 46, no. W1, pp. W257–W263, 2018, doi: 10.1093/nar/gky318.

[18] C. A. Lipinski, F. Lombardo, B. W. Dominy, and P. J. Feeney, "Experimental and computational approaches to estimate solubility and permeability in drug discovery and development settings," *Adv. Drug Deliv. Rev.*, vol. 64, no. SUPPL., pp. 4–17, 2012, doi: 10.1016/j.addr.2012.09.019.

[19] A. Toughzaoui, O. Chedadi, A. El Aissouq, Y. El Ouard, M. Bouachrine, A. Ouammou, *et al.*, "In silico studies of N-(4-tert-butylphenyl)-4-(3-chloropyridin-2-yl) piperazine-1-carboxamide derivatives as potent TRPV1 antagonists using 3D QSAR, ADMET and Molecular Docking," pp. 1–13, 2023, https://doi.org/10.21203/rs.3.rs-2962717/v1.

[20] E. A. Voight *et al.*, "Research & Development, AbbVie Inc., 1 North Waukegan Road, North Chicago, Illinois 60064, United States," vol. 1, 2014.

[21] L. W. Padgett, A. C. Howlett, and J. Y. Shim, "Binding mode prediction of conformationally restricted anandamide analogs within the CB1 receptor," *J. Mol. Signal.*, vol. 3, pp. 1–19, 2008, doi: 10.1186/1750-2187-3-5.

[22] A. Daina, O. Michielin, and V. Zoete, "SwissADME: A free web tool to evaluate pharmacokinetics, drug-likeness and medicinal chemistry friendliness of small molecules," *Sci. Rep.*, vol. 7, no. March, pp. 1–13, 2017, doi: 10.1038/srep42717.

[23] M. J. F. J. *et al.*, "Gaussian 98, revision a. 7, Gaussian," Inc., Pittsburgh, PA, vol. 12, 1998.

[24] K. B. Wiberg and P. R. Rablen, "Comparison of atomic charges derived via different procedures," *J. Comput. Chem.*, vol. 14, no. 12, pp. 1504–1518, 1993, doi: 10.1002/jcc.540141213.

[25] T. Hua, K. Vemuri, M. Pu, L. Qu, G. Won Han, Y. Wu, *et al.*, "Crystal Structure of the Human Cannabinoid Receptor CB1," *Cell*, vol. 167, no. 3, pp. 750–762.e14, 2016, doi: 10.1016/j.cell.2016.10.004.

[26] R. Thomsen and M. H. Christensen, "MolDock: A new technique for high-accuracy molecular docking," *J. Med. Chem.*, vol. 49, no. 11, pp. 3315–3321, Jun. 2006, doi: 10.1021/jm051197e.

[27] E. F. F. Da Cunha, D. T. Mancini, and T. C. Ramalho, "Molecular modeling of the Toxoplasma gondii adenosine kinase inhibitors," *Med. Chem. Res.*, vol. 21, no. 5, pp. 590–600, May 2012, doi: 10.1007/s00044-011-9554-z.

[28] J. M. Yang and C. C. Chen, "GEMDOCK: A Generic Evolutionary Method for Molecular Docking," *Proteins*, vol. 55, no. 2, pp. 288–304, May 2004, doi: 10.1002/prot.20035.

[29] A. P. Guimarães, T. C. Costa, T. Castro, M. Nascimento, E. Fontes, K. S. Matos, D. Texeira, *et al.*, "Docking studies and effects of syn-anti isomery of oximes derived from pyridine imidazol bicycled systems as potential human acetylcholinesterase reactivators," *J. App. Biomed.*, vol. 9, no. 3, pp. 163–171, Jan. 2011, doi: 10.2478/v10136-009-0037-1.

[30] J. A. Arnott and S. L. Planey, "The influence of lipophilicity in drug discovery and design," *Expert Opin. Drug Discov.*, vol. 7, no. 10, pp. 863–875, 2012, doi: 10.1517/17460441.2012.714363.

[31] J. S. Delaney, "ESOL: Estimating aqueous solubility directly from molecular structure," *J. Chem. Inf. Comput. Sci.*, vol. 44, no. 3, pp. 1000–1005, 2004, doi: 10.1021/ci034243x.

[32] J. Ali, P. Camilleri, M. B. Brown, A. J. Hutt, and S. B. Kirton, "In silico prediction of aqueous solubility using simple QSPR models: The importance of phenol and phenol-like moieties," *J. Chem. Inf. Model.*, vol. 52, no. 11, pp. 2950–2957, 2012, doi: 10.1021/ci300447c.

[33] J. Ali, P. Camilleri, M. B. Brown, A. J. Hutt, and S. B. Kirton, "Revisiting the general solubility equation: In silico prediction of aqueous solubility incorporating the effect of topographical polar surface area," *J. Chem. Inf. Model.*, vol. 52, no. 2, pp. 420–428, 2012, doi: 10.1021/ci200387c.

[34] S. Cao, S. Xu, H. Wang, Y. Ling, J. Dong, R. Xia, *et al.*, "Nanoparticles: Oral delivery for protein and peptide drugs," *AAPS PharmSciTech*, vol. 20, no. 5, pp. 1–11, 2019, doi: 10.1208/s12249-019-1325-z.

[35] A. Daina and V. Zoete, "A BOILED-Egg to predict gastrointestinal absorption and brain penetration of small molecules," *ChemMedChem*, pp. 1117–1121, 2016, doi: 10.1002/cmdc.201600182.

[36] X. Liu, C. Chen, and B. J. Smith, "Progress in brain penetration evaluation in drug discovery and development," *J. Pharmacol. Exp. Ther.*, vol. 325, no. 2, pp. 349–356, 2008, doi: 10.1124/jpet.107.130294.

[37] J. Kirchmair, A. Göller, D. Lang, J. Kunze, B. Testa, I. Wilson, *et al.*, "Predicting drug metabolism: Experiment and/or computation?" *Nat. Rev. Drug Discov.*, vol. 14, no. 6, pp. 387–404, 2015, doi: 10.1038/nrd4581.

[38] R. A. B. van Waterschoot and A. H. Schinkel, "A Critical Analysis of the Interplay between Cytochrome P450 3A and P-Glycoprotein: Recent insights from knockout and transgenic mice," *Pharmacological Reviews*, vol. 63, no. 2, pp. 390–410, 2011, doi: 10.1124/pr.110.002584.

[39] D. F. Veber, S. R. Johnson, H. Cheng, B. R. Smith, K. W. Ward, and K. D. Kopple, "Molecular Properties That Influence the Oral Bioavailability of Drug Candidates," *J. Med. Chem.*, vol. 45, pp. 2615–2623, 2002, doi: 10.1021/jm020017n.

[40] A. K. Ghose, V. N. Viswanadhan, and J. J. Wendoloski, "A Knowledge-Based Approach in Designing Combinatorial or Medicinal Chemistry Libraries for Drug Discovery. 1. A Qualitative and Quantitative Characterization of Known Drug Databases," *J. Comb. Chem.*, vol. 1, pp. 55–68, 1999, doi: 10.1021/cc9800071.

[41] I. Muegge, S. L. Heald, and D. Brittelli, "Simple selection criteria for drug-like chemical matter," *J. Med. Chem.*, vol. 44, no. 12, pp. 1841–1846, 2001, doi: 10.1021/jm015507e.

[42] W. J. Egan, K. M. Merz, and J. J. Baldwin, "Prediction of drug absorption using multivariate statistics," *J. Med. Chem.*, vol. 43, no. 21, pp. 3867–3877, 2000, doi: 10.1021/jm000292e.

[43] A. M. Rabasco Alvarez, "Biofarmacia y Farmacocinética Básica," *Avances en Farmacología y Farmacoterapia: Conceptos Básicos en Farmacología.*, pp. 32–56, 2002. [Online]. Available: http://dica.minec.gob.sv/inventa/attachments/article/3354/Biofarm-Farmacoc.pdf

Supplementary Material
Análisis ADMET

Table S1. Lipophilicity of the 30 compounds.

Molecule	TPSA	iLOGP	XLOGP3	WLOGP	MLOGP	Silicos-IT Log P	Consensus Log P
1	103,7	1,84	1,62	1,45	0,22	2,62	1,55
2	103,7	2,04	2,34	1,66	0,46	2,99	1,90
3	103,7	1,82	2,34	1,66	0,46	2,99	1,86
4	101,65	2,99	1,72	1,40	0,54	2,62	1,86
5	179,41	1,84	2,35	1,72	0,33	2,41	1,73
6	157,90	1,02	1,27	1,13	-0,02	1,72	1,02
7	164,11	3,00	2,47	2,43	1,02	2,40	2,27
8	142,88	2,54	3,50	3,34	0,66	3,64	2,74
9	97,35	2,25	1,40	1,41	1,21	1,70	1,59
10	108,21	2,48	1,25	1,48	0,40	2,75	1,67
11	79,11	2,69	2,65	2,75	1,08	3,46	2,53
12	49,33	2,55	3,04	2,41	2,36	3,19	2,71
13	49,33	2,47	3,04	2,41	2,36	3,19	2,69
14	116,09	2,48	3,86	3,39	2,26	3,55	3,11
15	116,09	2,14	3,86	3,39	2,26	3,55	3,04
16	86,63	2,68	2,00	1,81	1,11	3,05	2,13
17	86,63	2,48	2,54	2,20	1,36	3,46	2,41
18	86,63	2,78	3,08	2,59	1,60	3,87	2,78
19	92,42	2,60	1,74	1,77	1,11	2,81	2,01
20	92,42	2,87	2,28	2,16	1,36	3,22	2,38
21	92,42	3,13	2,82	2,55	1,60	3,63	2,75
22	89,79	2,39	1,88	1,33	1,20	2,73	1,91
23	89,79	2,36	2,43	1,72	1,44	3,14	2,22
24	89,79	2,60	2,97	2,11	1,68	3,55	2,58
25	89,79	2,59	1,88	1,33	1,20	2,73	1,95
26	89,79	2,51	2,43	1,72	1,44	3,14	2,25
27	89,79	2,23	2,97	2,11	1,68	3,55	2,51
28	95,58	3,07	2,71	2,08	1,68	3,31	2,57
29	95,58	2,82	2,71	2,08	1,68	3,31	2,52
30	113,34	1,80	0,80	-0,43	0,21	-0,23	0,43

Table S2. Solubility of the 30 compounds.

Molecule	ESOL Log S	ESOL Class	Ali Log S	Ali Class	Silicos-IT LogSw	Silicos-IT Class
1	-2.31	Soluble	-3.41	Soluble	-3.95	Soluble
2	-2.97	Soluble	-4.16	Moderately soluble	-4.19	Moderately soluble
3	-2.97	Soluble	-4.16	Moderately soluble	-4.19	Moderately soluble
4	-2.39	Soluble	-3.47	Soluble	-4.38	Moderately soluble
5	-3.59	Soluble	-5.76	Moderately soluble	-4.62	Moderately soluble
6	-2.91	Soluble	-4.18	Moderately soluble	-4.59	Moderately soluble
7	-3.85	Soluble	-5.56	Moderately soluble	-5.23	Moderately soluble
8	-4.38	Moderately soluble	-6.18	Poorly soluble	-5.77	Moderately soluble
9	-2.39	Soluble	-3.05	Soluble	-3.91	Soluble
10	-2.29	Soluble	-3.12	Soluble	-4.74	Moderately soluble
11	-3.08	Soluble	-3.96	Soluble	-4.71	Moderately soluble
12	-3.09	Soluble	-3.74	Soluble	-4.30	Moderately soluble
13	-3.09	Soluble	-3.74	Soluble	-4.30	Moderately soluble
14	-4.41	Moderately soluble	-5.99	Moderately soluble	-5.27	Moderately soluble
15	-4.41	Moderately soluble	-5.99	Moderately soluble	-5.27	Moderately soluble
16	-2.47	Soluble	-3.45	Soluble	-4.41	Moderately soluble
17	-2.82	Soluble	-4.01	Moderately soluble	-4.81	Moderately soluble
18	-3.17	Soluble	-4.57	Moderately soluble	-5.21	Moderately soluble
19	-2.30	Soluble	-3.30	Soluble	-4.63	Moderately soluble
20	-2.65	Soluble	-3.86	Soluble	-5.02	Moderately soluble
21	-3.00	Soluble	-4.42	Moderately soluble	-5.42	Moderately soluble
22	-2.41	Soluble	-3.39	Soluble	-3.93	Soluble
23	-2.77	Soluble	-3.96	Soluble	-4.33	Moderately soluble
24	-3.12	Soluble	-4.52	Moderately soluble	-4.73	Moderately soluble
25	-2.41	Soluble	-3.39	Soluble	-3.93	Soluble
26	-2.77	Soluble	-3.96	Soluble	-4.33	Moderately soluble
27	-3.12	Soluble	-4.52	Moderately soluble	-4.73	Moderately soluble
28	-2.95	Soluble	-4.37	Moderately soluble	-4.95	Moderately soluble
29	-2.95	Soluble	-4.37	Moderately soluble	-4.95	Moderately soluble
30	-2.68	Soluble	-2.76	Soluble	-3.06	Soluble

Table S3. Pharmacokinetic properties results.

Mol.	GI abs.	BBB perm.	Pgp sub.	CYP1A2 inh.	CYP2C19 inh.	CYP2C9 inh.	CYP2D6 inh.	CYP3A4 inh.	log Kp (cm/s)
1	High	No	No	No	No	No	No	No	-7.02
2	High	No	No	No	No	No	No	No	-6.72
3	High	No	No	No	No	No	No	No	-6.72
4	High	No	No	No	No	No	No	No	-7.05
5	Low	No	Yes	No	No	No	No	No	-7.44
6	Low	No	Yes	No	No	No	No	No	-7.83
7	Low	No	Yes	No	No	No	No	No	-7.50
8	Low	No	No	Yes	No	No	Yes	No	-6.33
9	High	No	Yes	No	No	No	No	No	-7.24
10	High	No	Yes	No	No	No	No	No	-7.35
11	High	No	No	Yes	No	No	Yes	No	-6.01
12	High	Yes	Yes	Yes	No	No	Yes	No	-5.66
13	High	Yes	Yes	No	No	No	Yes	No	-5.66
14	High	No	Yes	No	No	Yes	No	No	-6.01
15	High	No	Yes	No	No	No	No	No	-6.01
16	High	No	No	No	No	No	No	No	-6.67
17	High	No	No	No	No	No	No	No	-6.37
18	High	No	No	No	No	No	No	No	-6.07
19	High	No	No	No	No	No	No	No	-6.85
20	High	No	No	No	No	No	Yes	No	-6.55
21	High	No	No	No	No	No	Yes	Yes	-6.25
22	High	No	No	No	No	No	No	No	-6.77
23	High	No	Yes	No	No	No	No	No	-6.46
24	High	No	Yes	No	No	No	No	No	-6.16
25	High	No	No	No	No	No	No	No	-6.77
26	High	No	Yes	No	No	No	Yes	No	-6.46
27	High	No	Yes	No	No	No	No	No	-6.16
28	High	No	Yes	No	No	No	Yes	No	-6.34
29	High	No	Yes	No	No	No	No	No	-6.34
30	High	No	Yes	Yes	No	No	No	No	-7.81

Table S4. Drug similarity results.

Molecule	Lipinski #violations	Ghose #violations	Veber #violations	Egan #violations	Muegge #violations	Bioavailability Score
1	0	0	0	0	0	0.55
2	0	0	0	0	0	0.55
3	0	0	0	0	0	0.55
4	0	0	1	0	0	0.55
5	1	0	2	1	2	0.55
6	1	0	1	1	2	0.55
7	0	1	2	1	1	0.55
8	1	0	1	1	1	0.55
9	0	0	0	0	0	0.55
10	0	0	0	0	0	0.55
11	0	0	0	0	0	0.55
12	0	0	0	0	0	0.55
13	0	0	0	0	0	0.55
14	0	0	0	0	0	0.55
15	0	0	0	0	0	0.55
16	0	0	0	0	0	0.55
17	0	0	1	0	0	0.55
18	0	0	1	0	0	0.55
19	0	0	0	0	0	0.55
20	0	0	1	0	0	0.55
21	0	0	1	0	0	0.55
22	0	0	0	0	0	0.55
23	0	0	1	0	0	0.55
24	0	0	1	0	0	0.55
25	0	0	0	0	0	0.55
26	0	0	1	0	0	0.55
27	0	0	1	0	0	0.55
28	0	0	1	0	0	0.55
29	0	0	1	0	0	0.55
30	0	1	0	0	0	0.55

Table S5. Toxicity to the organism.

Molecule	Hepatotoxicity	Carcinogenicity	Mutagenicity	Cytotoxicity	Class
1	0.85	0.69	0.83	0.66	4
2	0.85	0.72	0.82	0.67	4
3	0.85	0.72	0.82	0.67	4
4	0.69	0.62	0.97	0.93	4
5	0.81	0.73	0.84	0.69	4
6	0.86	0.68	0.71	0.65	4
7	0.81	0.66	0.72	0.58	4
8	0.75	0.65	0.65	0.57	4
9	0.80	0.70	0.71	0.63	3
10	0.77	0.70	0.71	0.76	4
11	0.72	0.67	0.68	0.61	3
12	0.90	0.65	0.76	0.75	4
13	0.90	0.65	0.76	0.75	4
14	0.85	0.65	0.79	0.70	5
15	0.85	0.65	0.79	0.70	5
16	0.87	0.68	0.82	0.67	4
17	0.87	0.68	0.82	0.70	4
18	0.87	0.68	0.82	0.70	4
19	0.81	0.70	0.80	0.68	4
20	0.82	0.69	0.80	0.71	4
21	0.82	0.69	0.80	0.71	4
22	0.85	0.70	0.80	0.73	4
23	0.85	0.70	0.81	0.77	4
24	0.85	0.70	0.81	0.77	4
25	0.85	0.70	0.80	0.73	4
26	0.85	0.70	0.81	0.77	4
27	0.85	0.70	0.81	0.77	4
28	0.79	0.71	0.79	0.71	4
29	0.79	0.71	0.79	0.71	4
30	0.88	0.62	0.66	0.99	4

Molecular docking

Table S6. Energy score in Kcal/mol and hydrogen bridges formed by CB1.

Ligand	Intermolecular interaction energy (kcal/mol)	Amino acid residues	Strength (kcal/mol)	Bond length (Å)
1	-48.36	Thr197	-2.50	3.050
		Thr197	-0.019	3.490
		Thr197	-2.36	3.128
		Ala380	-0.80	3.441
2	-49.62	Ser383	-1.08	2.430
		Ser383	-2.50	2.926
		Ser123	-2.50	3.044
3	-68.23	Ser383	-1.14	3.372
		Ser383	-0.76	3.449
4	-51.85	Met103	-1.03	2.426
		Gln116	-2.50	2.638
		His178	-2.50	2.971
		Met103	-0.27	3.545
5	-73.99	Ala120	-0.0051	3.501
		Gly166	-0.44	3.513
		Phe170	-1.06	2.694
		Ser173	-0.26	3.549
		Met103	-1.75	3.023
6	-5.24	Phe108	-0.96	3.322
		Phe108	-0.92	2.410
		Ser383	-1.20	3.360
		Cys386	-2.29	3.143
7	+4.66	Trp279	-0.41	3.406
		Thr197	-0.11	3.372
		Thr197	-2.50	2.718
8	-73.74	Thr197	-0.011	3.456
		Trp279	-1.04	3.102
		Phe170	-0.49	2.635
9	-96.27	Ser383	-2.50	3.025
10	-97.51	Thr197	-2.36	2.952
		Leu193	-0.20	3.560
11	-80.58	–	–	–
12	-91.04	Cys386	-1.49	3.303
		Ser 390	-0.71	3.459
13	-77.13	–	–	–
14	-66.47	Ser383	-0.41	3.334
15	-42.06	Thr197	-2.50	2.894
		Ser383	-2.25	3.150
16	-81.85	Ile267	-1.87	3.227
		Ser383	-0.66	2.446
17	-88.67	–	–	–
18	-41.85	–	–	–
19	-94.96	–	–	–

Ligand	Intermolecular interaction energy (kcal/mol)	Amino acid residues	Strength (kcal/mol)	Bond length (Å)
20	-79.13	Pro265	-1.56	3.287
		Ser383	-2.50	2.791
		Asp104	-0.41	2.472
		Met103	-1.47	2.833
21	-87.21		-0.68	3.315
		Thr197	-0.79	2.394
22	-91.37	Ala380	-1.98	2.851
23	-104.45	Ser383	-2.50	3.045
		Ser123	-2.50	2.745
24	-98.60	Ala380	-2.31	3.139
		Ser383	-0.89	3.422
		Ser390	-2.50	2.974
25	-92.66	Asp163	-1.19	3.361
		Asp104	-2.50	3.027
		Ser123	-2.50	2.800
26	-69.66	Ser383	-1.89	2.718
		Asn101	-2.50	2.764
		Asp104	-2.25	2.886
		Met103	-0.57	2.862
27	-45.84	Pro269	-2.50	2.646
		Ser383	-2.38	2.586
		Ala380	-1.52	3.296
28	-92.88	–	–	–
29	-97.70	Ala380	-0.21	3.287
30	-118.91	Ile267	-1.31	3.338
		Asp104	-0.11	3.419